

Climate links and recent extremes in antarctic sea ice, high-latitude cyclones, Southern Annular Mode and ENSO

Alexandre Bernardes Pezza · Harun A. Rashid · Ian Simmonds

Received: 15 June 2010 / Accepted: 5 March 2011 / Published online: 16 March 2011
© Springer-Verlag 2011

Abstract In this article, we study the climate link between the Southern Annular Mode (SAM) and the southern sea-ice extent (SIE), and discuss the possible role of stationary waves and synoptic eddies in establishing this link. In doing so, we have used a combination of techniques involving spatial correlations of SIE, eddy streamfunction and wind anomalies, and statistics of high-latitude cyclone strength. It is suggested that stationary waves may be amplified by eddy anomalies associated with high latitude cyclones, resulting in more sea ice when the SAM is in its positive phase for most, but not all, longitudes. A similar association is observed during ENSO (La Niña years). Although this synergy in the SAM/ENSO response may partially reflect preferential areas for wave amplification around Antarctica, the short extent of the climate records does not allow for a definite causality connection to be established with SIE. Stronger polar cyclones are observed over the areas where the stationary waves are amplified. These deeper cyclones will break up and export ice equatorward more efficiently, but the near-coastal regions are cold enough to allow for a rapid re-freeze of the resulting ice break-up. We speculate that if global warming continues this same effect could help reverse the current (positive) Antarctic SIE trends once the ice gets thinner, similarly to what has been observed in the Northern Hemisphere.

Keywords Sea ice · Antarctica · Southern Annular Mode · El Niño · Mid-latitude storms · Cyclones

1 Introduction

Changes in sea ice extent (SIE) can influence the global energy balance through changes in enthalpy fluxes and albedo, while changes in the meridional temperature gradient can alter the atmospheric eddy activity which accounts for most of the heat exchange in the oceans and in the atmosphere (Simmonds and Wu 1993; Raphael 2003; Holland and Raphael 2006). Sea ice has numerous effects on the Southern Hemisphere (SH) climate. Its insulation helps to preserve ocean heat affecting the ocean currents and the climate balance (Yuan and Martinson 2000; Raphael 2003). It is evident that the ice/atmosphere system is characterised by complex feedback interactions.

Several papers over the last two decades have explored the impact of sea ice changes on the SH atmospheric circulation (e.g., Simmonds and Budd 1991; Simmonds and Wu 1993; Godfred-Spenning and Simmonds 1996; Simmonds 2003a; Parkinson 2004; Simmonds et al. 2005; Pezza et al. 2008), while many others have shown that atmospheric forcing is fundamental to explain the general sea ice behaviour (e.g., Uotila et al. 2000; Uotila 2001; Hall and Visbeck 2002; Kwok and Comiso 2002; Lefebvre et al. 2004; Yuan and Li 2008). A number of other studies have also explored the spatial and temporal variations of the SIE and their relationships with various indices of climate variability, particularly indices of ENSO (El Niño-Southern Oscillation) and of the annular modes (Simmonds and Jacka 1995; Kwok and Comiso 2002; Hall and Visbeck 2002; Simmonds 2003b; Turner 2004; Liu et al. 2004; Lefebvre et al. 2004; Yuan and Li 2008; Stammerjohn et al. 2008).

A. B. Pezza (✉) · I. Simmonds
School of Earth Sciences, The University of Melbourne,
Parkville, VIC 3010, Australia
e-mail: apezza@unimelb.edu.au

H. A. Rashid
Centre for Australian Weather and Climate Research
(A partnership between CSIRO and the Bureau of Meteorology),
Private Bag 1, Melbourne, VIC 3195, Australia

Fogt and Bromwich (2006) explore the large scale teleconnections between ENSO and high latitudes, showing that an in-phase relationship with the Pacific-South American (PSA) pattern has the ability to increase the correlations between ENSO and the Southern Annular Mode (SAM), suggesting that the tropical and high latitudes need to work together in order for ENSO to strongly influence Antarctic climate.

An interesting aspect of sea ice is the sharp contrast in behaviour in the two Hemispheres in recent decades. While in the SH there has been a modest increasing trend over the satellite period (Watkins and Simmonds 2000; Zwally et al. 2002; Parkinson 2004, Turner et al. 2007; Comiso and Nishio 2008), the Northern Hemisphere (NH) has had a substantial decline in sea ice which has been at least partially attributed to global warming (Rothrock et al. 1999; Stroeve et al. 2005, 2007; Serreze et al. 2003, 2007; IPCC 2007; Simmonds et al. 2008; Comiso and Nishio 2008; Simmonds and Key 2009).

The annular modes (Gong and Wang 1999; Fyfe et al. 1999; Thompson and Wallace 2000) can be partially associated with the SIE variability. While the SAM has shown a significant trend towards its positive phase over the SH summer during the satellite era (Thompson and Solomon 2002; Marshall 2003; Fogt et al. 2009), the Northern Annular Mode (NAM) and North Atlantic Oscillation (NAO) have shown a variable pattern that cannot fully explain the recent decline in northern sea ice (Hurrell 1995; Thompson et al. 2000; Cohen and Barlow 2005; Wang et al. 2009). The SAM's trend during the SH summer has been at least partially induced by ozone depletion, as well as increased greenhouse gas concentration (Thompson and Solomon 2002; Renwick 2004; Shindell and Schmidt 2004; Cai et al. 2005; Roscoe and Haigh 2007; Kidston et al. 2009). Fogt et al. (2009) argue that the summer trend in the SAM is the only season that can be robustly attributed as having a trend outside the range of natural climate variability. It is unclear how the SAM will respond to a recovery to pre-industrial stratospheric ozone concentrations and to changes in sea ice.

The developments above suggest that a complete understanding of the feedback mechanisms driving the annular modes and the sea ice in both hemispheres is still lacking, particularly as these mechanisms involve transient eddies and structure of the large scale circulation. The variability of mesoscale cyclones commonly observed over the ice edge such as polar lows, and other synoptic and mesoscale cyclones, is of importance for continental mid-latitude precipitation in the SH. An advance in our understanding of this scale interaction in a context of changing SAM and SIE is needed to help clarify many details of the polar and mid-latitude climates. Of direct interest is the persistent drought tendency in the SH (low

mid-latitudes over the last decades, for which south-eastern Australia offers a dramatic example (e.g., Lovenduski and Gruber 2005; Meneghini et al. 2007; Hendon et al. 2007; Herweijer and Seager 2008).

In this paper we discuss the link between the SAM and southern sea ice, and the influence of stationary waves and transient eddies on this link. We advance from recent findings (Kwok and Comiso 2002; Lefebvre et al. 2004; Stammerjohn et al. 2008; Yuan and Li 2008; Wheeler 2008) by addressing why the sea ice response to SAM displays zonal asymmetry, how this is similar to the climate signal associated with ENSO (L'Heureux and Thompson 2006) and how the spatially inhomogeneous response is shaped by transient eddies (synoptic and mesoscale cyclones). New insights on the role of intense sub-polar cyclones in pushing the ice edge further north, and in reinforcing stationary wave structures that are recurrently seen at preferential longitudes during both SAM and ENSO extreme periods are discussed. Relatively little is known of the ice feedback mechanisms involving SAM/ENSO, and to what extent they can be regarded independently as there are many non-linear effects which affect them both (Khokhlov et al. 2006; Karpechko et al. 2009). Our work also advances on the recent trends (Comiso and Nishio 2008) and the very different southern sea ice behaviour compared to the NH, discussing the extreme southern anomalies observed in the summer 2008. We start with recent trends in SAM and SIE in Sect. 3.1, followed by large scale associations in 3.2. In Sect. 3.3 cyclone behaviour is discussed with emphasis on the interaction between the transient eddies and SIE/SAM via wave amplification, followed by a case study for the summer 2008 discussed in a climate perspective in 3.4.

2 Materials and methods

We have used two definitions of the SAM. Their temporal variations are strongly correlated (correlation coefficient 0.89) and each has specific advantages depending on the type of analysis. The first is defined as the leading Empirical Orthogonal Function (EOF) of vertically-averaged (1000–175 hPa) geostrophic streamfunction (ψ) anomalies over the SH extratropics poleward of 20°S, and the corresponding principal component (PC) was employed for the climatological study of the associations with SIE. A second index of the SAM, employed in the cyclone behaviour analysis, was the National Oceanic and Atmospheric Administration (NOAA) 700 hPa reanalysis-derived Antarctic Oscillation Index (AAOI). This definition of the AAOI is readily available, making it easy for our cyclone composites to be compared with future studies and used as a reference. The AAOI can also be defined in terms of station

data, presenting a slightly different perspective on the SAM. We use standard (unrotated) EOFs calculated from the area-weighted ψ anomalies. As an index of ENSO we use the deseasonalized SST time series averaged over the Niño 3.4 region (bounded by 120–170°W and 5°S–5°N).

For the analysis presented in this paper we use the sea ice extent and atmospheric circulation data for the period 1979–2008, except for sea-ice edge data, which is available up to 2000. Atmospheric data from the NCEP2 reanalysis (Kanamitsu et al. 2002) were used for most of the calculations involving pressure, geopotential height and winds. The results were also compared to the ERA40 and JRA25 reanalysis (Uppala et al. 2005 and Onogi et al. 2007 respectively), and show that the general spatial outlook and trends are very similar amongst the different datasets. The JRA25 dataset offers a slightly more refined spatial structure of cyclones around Antarctica, and has an enhanced potential to capture polar lows (Uotila et al. 2009). For this reason we have used it for the analyses pertaining to cyclone behaviour.

SIE derived from remotely sensed Nimbus-7 SMMR and DMSP SSM/I passive microwave data from the National Aeronautics and Space Administration's (NASA's) National Snow and Ice Data Center (NSIDC) is used. This data set includes daily and monthly averaged sea ice concentrations at a grid cell size of 25×25 km. In computing the total sea ice extent, pixels must have an ice concentration of 15% or greater to be included. The total SIE is then calculated by summing up the number of pixels with at least 15% ice concentration multiplied by the total pixel area (Gloersen et al. 1992).

Cyclone properties were obtained through the Melbourne University tracking algorithm (e.g., Murray and Simmonds 1991; Jones and Simmonds 1993; Simmonds and Keay 2000; Simmonds et al. 2003). From the statistical component of the software we used cyclone System Density (SD) and Depth (DP). SD is defined as the average number of cyclones/anticyclones within a reference area of 10^3 (deg.lat)², which is here referred to as SD unit. The DP is proportional to the Laplacian of the MSLP and can be seen as the MSLP difference between the “edge” and the center of the system (Simmonds et al. 2003; Lim and Simmonds 2007). In addition to the obvious value of a synoptic indicator, this measure has the advantage of being relatively insensitive to artificial trends in the MSLP which might exist in the reanalysis.

Composites of cyclone SD and DP were calculated for positive and negative AAOI and SIE anomalies using the criterion of the top five and bottom five anomalous years. This is equivalent to choosing anomalous cases away from the mean by about one and a half standard deviations, but with the advantage of having the same number of years for each composite. The difference maps between top and

bottom cases are presented to maximize the signal in areas that have opposite responses for different SAM/SIE polarities.

3 Results

3.1 Spatial asymmetries and recent trends

Figure 1 shows the leading EOF of the vertically-averaged geostrophic streamfunction anomalies computed over the SH south of 20°S using all months of the year. The EOF was computed from monthly mean data after removing the climatological annual cycle (defined as the long-term means of individual months over 1979–2008). In Fig. 1a, a clearly asymmetric structure, superposed on an annular mode pattern, is seen south of 50°S, with three major mid-latitude nodes in the western Atlantic, Indian and western Pacific oceans. This asymmetric pattern is more pronounced during winter (Kidston et al. 2009), and is a key component of the climatic variability in the SH. As discussed in the next sections, this variability is also accompanied by a shift in the sea ice field. The longitudinal variations have the largest amplitudes in the South Pacific sector and project strongly onto zonal wavenumbers 1–3.

The wave amplitudes mentioned above are displayed in Fig. 1b which shows the latitudinal distribution of the Fourier amplitudes as a function of the zonal wavenumber associated with the leading EOF. The amplitudes were computed by Fourier analyses around latitude circles of the EOF spatial pattern in Fig. 1a. We see that the amplitudes are largest between 50 and 70°S, with lower wavenumbers dominant at high and subtropical latitudes, and higher wavenumbers occurring at mid-latitudes. Any potential perturbation in the climate system associated with the SAM will also generate anomalies for which the wavenumber will be latitude dependent. Most of the area on the interface between the sea ice and open waters lies over latitudes for which the maximum energy is dispersed onto waves of wavenumbers 1 and 2.

Figure 2 shows two indices of the SAM: the SAM index, based on the vertically-averaged geostrophic streamfunction (Fig. 2a) and the AAO index, derived from the 700-hPa height analysis (Fig. 2b). The SAM has irregular temporal variability with the largest variance found at the longest timescales, consistent with a low-order auto-regressive process (Rashid and Simmonds 2004). There is very little trend in the two indices when the entire data period (1979–2008) is considered. However, a piecewise trend analysis of the indices for the sub-periods 1979–1991, 1992–2001, and 2002–2008 shows a different picture. There is no detectable trend seen during 1979–1991, whereas an upward trend is detected during

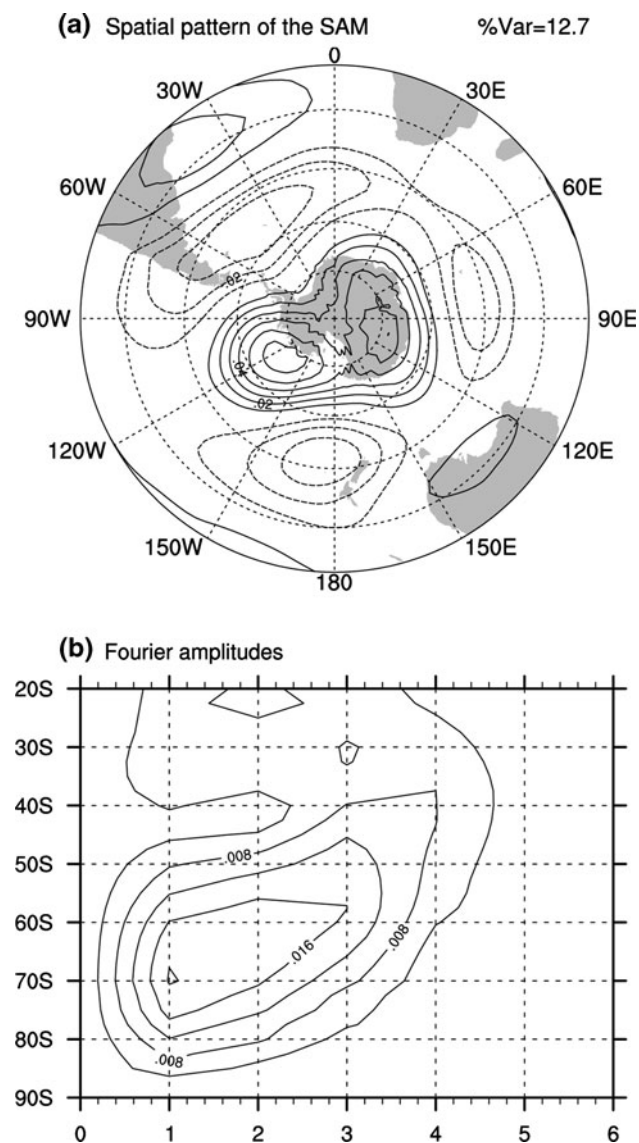


Fig. 1 a The leading Empirical Orthogonal Function of the vertically-averaged geostrophic streamfunction anomalies calculated over the domain 20° – 90° S and 0° – 360° E using all months of the year, period 1979–2008 and (b) the Fourier amplitudes of the EOF pattern, computed by Fourier analyses around latitude circles

1992–2001 and 2002–2008. The last two sub-periods were chosen to separate the SAM index before and after a major shift in the index in 2002, associated with a breakdown of the stratospheric polar vortex (Krüger et al. 2005; Mbatha et al. 2010). This increasing positive polarity, which has been more pronounced over the SH late spring and early summer, has been associated, in part, with global warming and ozone losses (Thompson and Solomon 2002; Renwick 2004; Shindell and Schmidt 2004; Cai et al. 2005; Roscoe and Haigh 2007).

We now discuss the recent trends in the SAM (using the AAOI) and in SIE on a seasonal basis, to complement the results shown in Fig. 2 for different sub-periods. Figure 3

shows the AAOI measured over the same period as in Fig. 2, but for DJF and JJA. A significant positive trend (95%) is seen in summer and a weak negative trend is seen in winter. While the summer increase more closely resembles a shift towards the positive polarity in the last two decades (in agreement with our analyses in Fig. 2), the slight negative trend in winter would require a longer dataset to infer processes other than, possibly, the multi-decadal natural climate variability.

Figure 4 shows the southern SIE variability by season from autumn 1979 to autumn 2008. The linear trends are also plotted for comparison, but the squared correlation coefficient is given only for trends that are significant at or above 95%. The seasons SON and JJA have the greatest SIE with a total between 16 and 18×10^6 km², while DJF and MAM have the least extent. But even during the low ice season the SIE rarely drops below 6×10^6 km². Modest trends are observed during all seasons, with that in SON being statistically significant at level 95%. The absolute trends over spring and autumn are the most pronounced, with an increase of about half a million square kilometres over the whole period. In percentage terms there is an increase between 2 and 3% during winter and spring and from 5 to 7% during the low ice season, with the greatest changes occurring in MAM. Although the trends are modest, the increase of up to 7% during the low ice season represents an additional input of ice into the system (or rather lack of melting) which is large enough to have a significant influence via changes in albedo and associated changes in cyclones (see Sect. 3.3). This pattern is very different to the behaviour observed in the NH, where strong declining trends have been increasingly associated with global warming (Rothrock et al. 1999; Stroeve et al. 2005, 2007; Serreze et al. 2003, 2007; IPCC 2007; Simmonds et al. 2008, Simmonds and Keay 2009 and references therein).

Figure 4 also shows that the greatest SIE on record observed during the low sea ice season occurred repeatedly in D2007–JF2008 (DJF2008) and MAM2008, far greater than the previous records. DJF2008 presented a SIE of about 6% greater than the previous record, whereas MAM2008 SIE stands at about 8% greater than any other year on record. This is substantial considering that the overall variability between record minimum and maximum extent prior to 2008 ranged at about 20% in both seasons. The summer and autumn trends weaken if 2008 is removed from the series but are still present, notwithstanding the fact that the most robust trend is seen in SON as discussed above.

While it is not straightforward to determine to what extent the trends in SIE and SAM may be connected, we will next offer a discussion and some new insights into the problem of large scale connections associated with sea ice

Fig. 2 **a** The SAM index, taken as PC of the leading EOF shown in Fig. 1a and **b** the AAO index, computed as PC of the leading EOF of 700-hPa geopotential height anomalies. The trends for 1979–1991, 1992–2001, and 2002–2008 were separately calculated. See text for further details

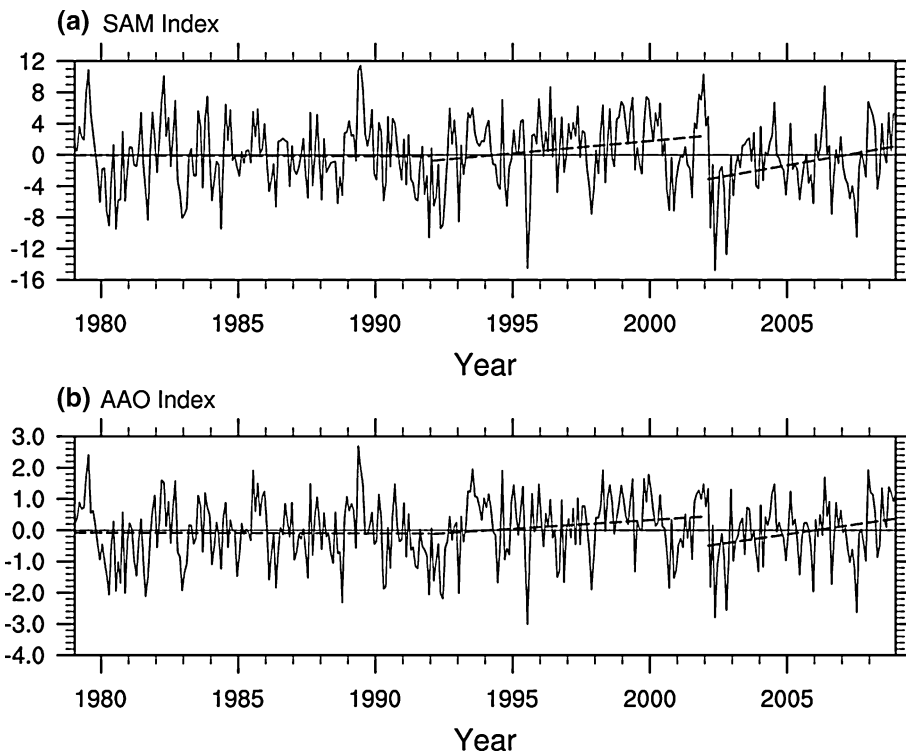
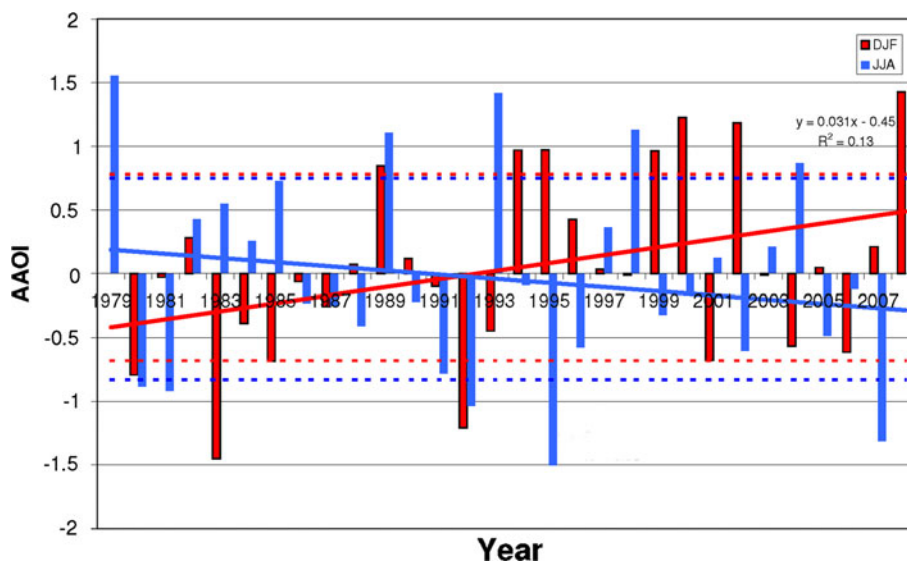


Fig. 3 700 hPa Antarctic Oscillation Index (AAOI) for June–July–August (JJA) and December–January–February (DJF) 1979–2008. The DJF dataset starts in 1980, and the JJA dataset finishes in 2007. The linear trends, squared correlation coefficients (where the trends are significant at or above 95%) and standard deviations are also shown



motion. In Sect. 3.3 the role of cyclones will be explored, implying that the regional ice will more closely follow the nuances of anomalous stationary wave pattern related to cyclone activity.

3.2 Large scale associations with ice motion

In this section the associations between the SAM, ENSO and SIE are explored. When invoking these relationships it is apparent that SAM and ENSO are interlinked in terms of their response observed in the sea ice field as well as cyclone

strength, mainly through non-linear effects (e.g., Khokhlov et al. 2006). As shown below, it is apparent that while over most of the longitudes the associations mirror each other there are also regions in which they are unique (e.g., there is a SAM influence and there is not an ENSO influence). We offer this discussion building on the recent literature where it is still unclear whether SAM and ENSO operate together in their response mechanism or if the final responses in the sea ice field are similar principally because of a preferred high latitude mode of stationary wave response all-around Antarctica. We argue here in favour of the latter.

Fig. 4 Total southern sea ice extent—SIE (10^6 km^2) given by season, period 1979–2008. Some seasons start in 1980 and some finish in 2007, and there is no data for the summer 1988. The linear trends and squared correlation coefficients (where the trends are significant at or above 95%) are also shown

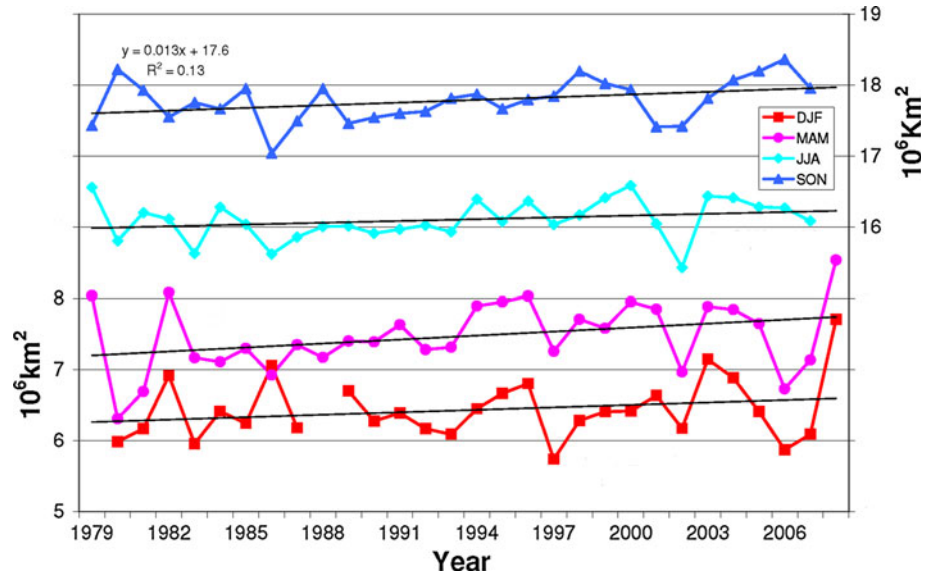


Figure 5 shows the climatological mean position of the SIE along with the total and the anomalous standard deviations calculated, respectively, from the monthly time series before and after filtering the seasonal cycle. The largest temporal variability occurs over the South Atlantic and central South Pacific, whereas over the Indian Ocean the variability is least. The longitudinal variability is a key part of the sea ice's seasonal cycle, and resembles the variability in the SAM. The regions of largest variability coincide with those sectors of the Southern Ocean (the Ross and Weddell Seas) where the oceanic areas penetrate further south, thereby allowing for greater north–south displacement of sea ice.

Figure 6 shows the correlation coefficients between the SAM index (continuous) and Niño 3.4 SST (dashed) and the latitudes of the SIE as a function of longitude. The seasonal cycle was removed from the monthly mean data before calculating the correlation coefficients. The thin light gray line represents the correlation when all data points in the corresponding time series pair are considered. The thick dark gray lines represent the correlation coefficients when only the data points exceeding the respective one standard deviation values are correlated with the time series of SIE latitudes.

For ENSO the largest correlations are found in the Bellingshausen Sea (positive) and South Pacific/Ross Sea (negative), in agreement with Simmonds and Jacka (1995), Kwok and Comiso (2002) and Renwick (2002). Other areas of moderate correlation occur in the Weddell Sea (positive) and in the Southern Ocean between the Atlantic and Indian Ocean sectors (negative). It is apparent that the blocking anticyclone formed over the far south-eastern Pacific during El Niño years (Renwick 1998, 2002) induces a southward ice retreat (negative

Climatological mean Sea-ice edge, and total and anomalous standard deviations

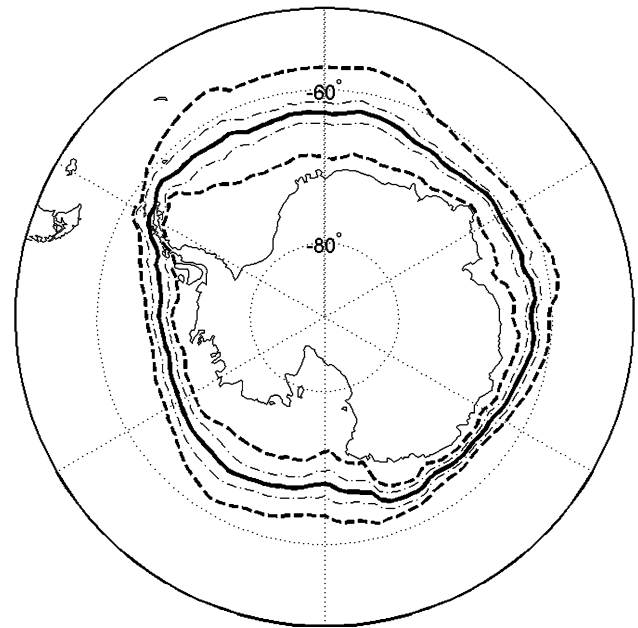
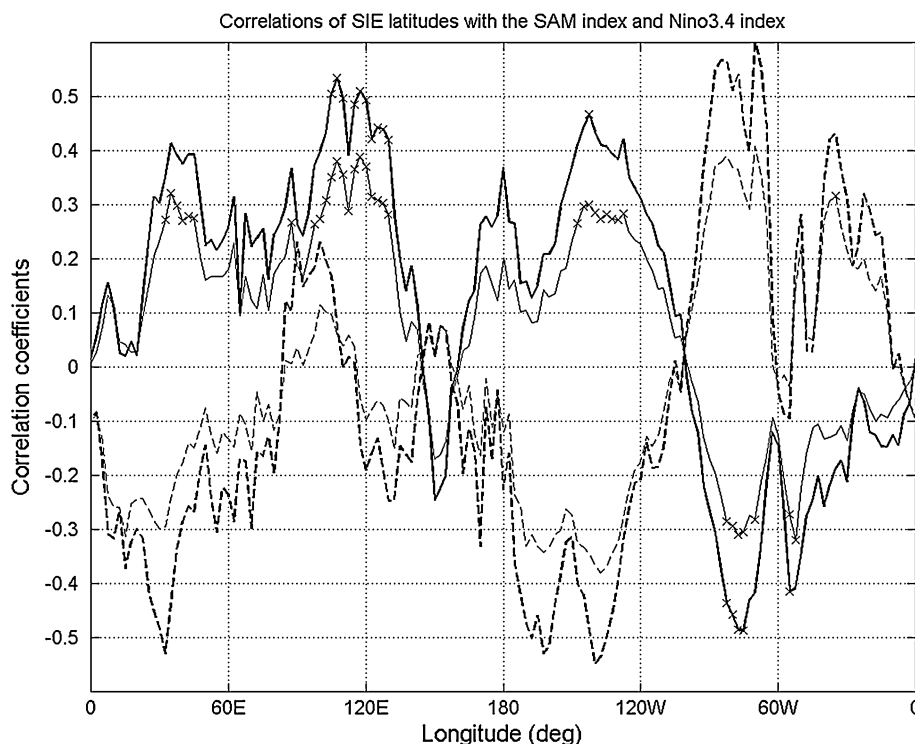


Fig. 5 Climatological mean sea-ice edge positions (*thick continuous line*) calculated over the period 1979–2000. Also shown in the figure are the total (*thick dashed lines*) and the anomalous standard deviations (*thin dash-dotted lines*) of sea-ice edge positioning

correlation) in the South Pacific and Ross Sea sections, and a northward forcing (positive correlation) in the Bellingshausen and Weddell Seas as seen in Fig. 6. This agrees with Renwick (2002), who suggested a combination of anomalous heat fluxes and direct advection to explain the sea ice variability.

For the SAM, the largest correlations occur in the southeast Indian Ocean, with values of about +0.5. This appears in a region where the sea ice and Niño 3.4 are

Fig. 6 Correlations of the SAM index (*continuous lines*) and of an index of El Niño/Southern Oscillation—ENSO (*dashed lines*) with sea ice extent latitudes at different longitudes. In each case, the *thin light gray line* represents the correlation coefficients when all the data points of the corresponding time series pair are considered. The *thick dark gray lines* represent the correlation coefficients when only the data points of the SAM index and ENSO index exceeding the respective one standard deviation value are correlated with the corresponding data points of the time series of SIE latitude. The points significant at 95% level are marked with an ‘x’ symbol. Period 1979–2000, all months of the year used. See text for further details



uncorrelated, suggesting that the SAM response is not a by-product of the association with ENSO. While this complementary relationship is consistent with the conceptual idea of a synergetic system involving SAM, ENSO and sea ice as recently suggested by Pezza et al. (2008), Stammerjohn et al. (2008) and Yuan and Li (2008), it also makes the case for a SAM-SIE interplay in the southwest of Australia which is unaffected by ENSO. We note that the SAM and ENSO curves to some extent mirror each other, but the extent to what they could be both responding to a common factor is still a matter of ongoing research. We suggest that SAM and ENSO are integrated as far as their large scale response is concerned, but the fact that their responses seem to project onto similar stationary modes in high latitudes cannot be used to say that they are the same. Often in nature two completely different processes may lead to similar results: the physical processes that generate ENSO and SAM are apparently very different. As discussed in Sect. 3.3 below, the cyclone and SIE spatial anomaly analysis also seem to suggest that there are certain areas of preferential activity around Antarctica where larger scale anomalies originating from ENSO and SAM would tend to manifest themselves in the form of stationary waves.

The sign of the correlations changes dramatically with longitude, which suggests that atmospheric processes may

be driving the changes in sea ice. The points that are significant at 95% are marked by an ‘x’ symbol in the figure. The significance levels are estimated by taking the respective autocorrelation into account (Lau et al. 1994). Note that the ENSO—SIE correlations are not significant at 95% level, as a result of ENSO’s longer persistence (therefore, smaller equivalent sample size). However, the correlations are still strong and tend to be larger than the corresponding SAM values. The lack of statistical significance at 95% level doesn’t prove that the ENSO correlations are not important, but perhaps rather that the sample is not large enough to prove or disprove the significance. In fact, the physical rationale for the statistical relationship is consistent with previous works (e.g., Kwok and Comiso 2002).

The curves form a longitudinal pattern that bears some resemblance to a wave number two. This wave-like pattern suggested by the correlations strongly mimics the eddy streamfunction anomalies associated with the SAM. It is also evident that the correlations taken when the indices exceed one standard deviation (thick lines) are stronger in all longitudes (while obviously having the significance reduced as a result of sample reduction), and this is maximized at the longitudes where the response is more pronounced. This behaviour points to nonlinearity (e.g., Simmonds and Hope 1997), and makes a stronger case that the correlations arise because of a physical association.

The correlations in Fig. 6 indicate that the SIE to the southwest of Australia tends to be greater than normal when the SAM is positive. This SIE region was shown to be negatively correlated with rainfall in Perth (south-western Australia) during the winter (Pezza et al. 2008), suggesting that positive SAM and greater sea ice are associated with reduced rainfall in south-western Australia (Hendon et al. 2007; Meneghini et al. 2007). Pezza et al. (2008) also showed that the cyclone anomalies observed during years of greater SIE resemble the cyclone anomalies observed during positive SAM years even when independent composites are calculated, i.e., using only SIE years that were not SAM years or vice versa. This brings us to the point discussed earlier that there seems to be areas of preferential wave anomaly trapped around Antarctica which arise in anomalous SIE years even in the absence of any apparent SAM or ENSO forcing.

Other areas where the correlation between the SAM and the SIE is significant are the Bellingshausen Sea (negative) and the South Pacific and southwestern Indian Oceans (positive). In those areas ENSO is also correlated to sea ice (although not reaching 95% significance), but with opposite sign. Over most of the South Indian Ocean and South Pacific the correlations imply that stronger high latitude westerlies are associated with a northward advancement of the ice. For the regions where the correlations are negative (e.g., the Bellingshausen and west Weddell Sea sectors) the SIE presents a southward retreat when stronger than normal westerlies occur.

The fact that the zonally-asymmetric SIE anomalies are associated with nearly zonally-symmetric fluctuations of the westerlies points to the importance of stationary waves (in the atmosphere) in this relationship. It is conceivable that temporal variations of the westerlies can influence the SIE positions indirectly through variations in the induced stationary wave trains. Such a mechanism incorporates the concept of how the wave trains organise around Antarctica. The concept of stationarity further implies a dependence on the landmass which would be particularly sensitive on the high elevations of the Antarctic Plateau, adding a new element to the observations made by Kwok and Comiso (2002) and Renwick (2002) for the interaction between the sea ice and the blocking anticyclones over high latitudes.

In Sects. 3.3 and 3.4 we will show that the cyclone intensity anomalies also follow a wave-like pattern that seems to support the hypothesis above. In particular, we will discuss that the spatial distribution of the cyclone anomalies seems to present little change regardless of the choice of composite being defined as a function of SAM or SIE extremes. Our results are also consistent with the calculations done by Lefebvre et al. (2004), and in particular with their Fig. 7 which gives a perspective on the spatial changes in sea ice concentration. We note that the relationships

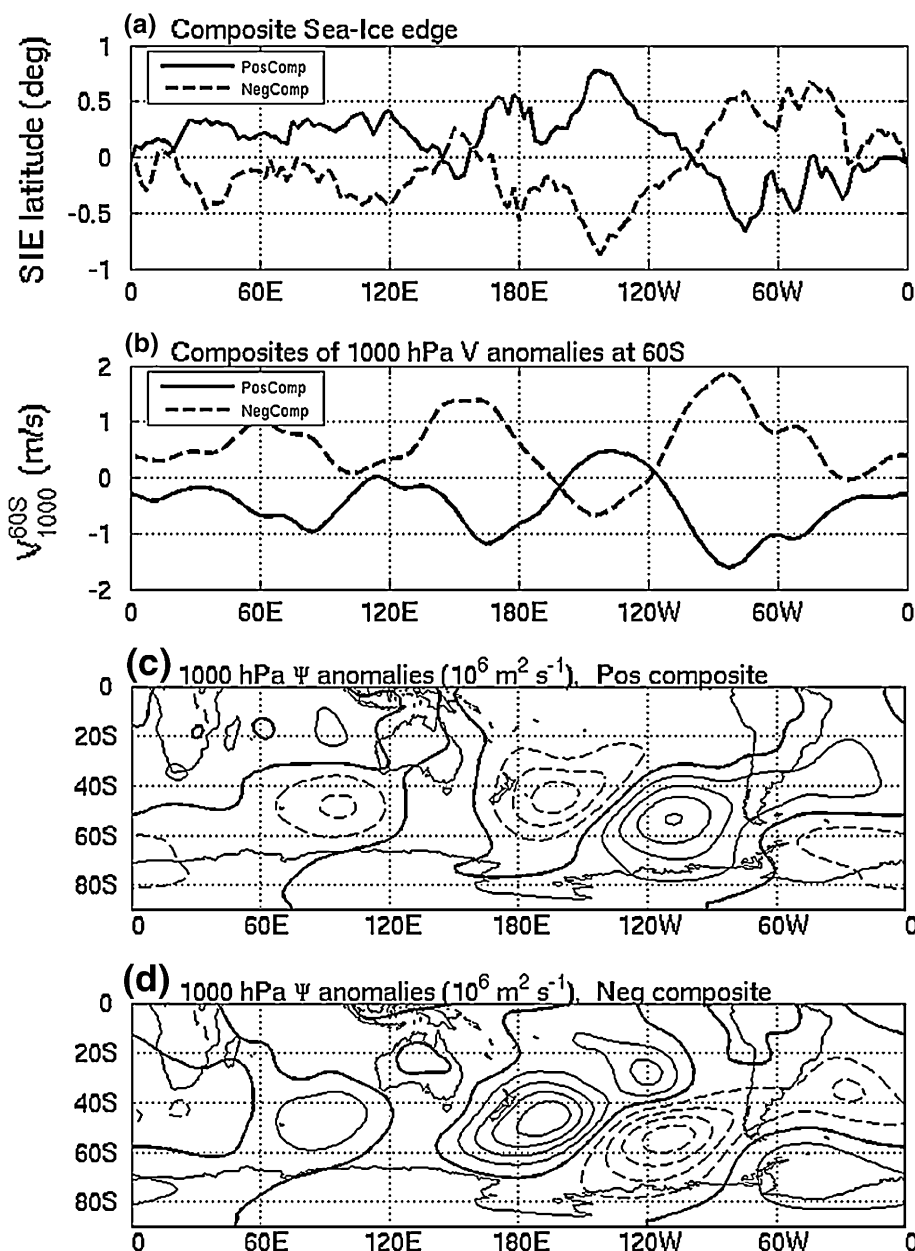
involving all months here discussed also hold, with only minor differences, for each season (not shown). One of the few regions around Antarctica that has a different SIE seasonal response is the Weddell Sea between summer and winter. This is discussed in Sect. 3.4 in light of the exceptional climate anomalies observed during the summer 2008.

To further elucidate the large scale connections associated with sea ice motion we present in Fig. 7 the composites of the 1000 hPa streamfunction anomalies for the positive (c) and negative (d) phases of the SAM. For ease of comparison, we also present the corresponding composites of SIE latitude anomalies in Fig. 7a and of the 1000-hPa meridional wind anomalies at 60°S in Fig. 7b. We note that this latitude falls near the sea ice/open water edge at most longitudes during the period of maximum SIE (see Fig. 5). The composites were calculated from SAM anomalies exceeding one standard deviation. The largest positive SIE anomalies (solid curve, Fig. 7a), located in the Pacific sector, coincide with the anomalous northward advection associated with the anticyclone-cyclone pair in that sector (Fig. 7c). Similarly, the largest negative SIE anomalies (dashed curve, Fig. 7a) coincide with the anomalous southward advection associated with the opposite streamfunction anomalies (Fig. 7d). The wave pattern strongly resembles the structure already inferred by the correlations in Fig. 6, which suggests that the stationary waves are at least partially driving the sea-ice anomalies.

Figure 7 also shows that the relationship between SIE and the meridional wind is weaker to the west of the date line, perhaps because this latitude band is too close to the Antarctic landmass over those longitudes and hence not very representative of the environment associated with free ice (Fig. 5). We must stress however that one would not expect the relationship between the wind given at a single latitude band and the SIE to be exact. There are obvious asymmetries in the average location of the sea ice in relation to the 60° latitude band in addition to the asymmetries in the shape of the Antarctic continent which has most of its landmass concentrated in the eastern hemisphere (Baines and Fraedrich 1989). In other words, the reference wind at 60°S should be thought as a parameter that helps validate the relationships proposed earlier, but it cannot and should not be interpreted as necessarily having a symmetrical (linear) relationship with SIE. Where such a relationship is found, though, we can confidently state that our proposed mechanism (i.e., stationary waves generating the wind anomalies that will impact the ice) could be verified.

In addition to the mechanism discussed above, Fig. 7c, d also show that the amplitude of the waves is greater in the western hemisphere and that the latitude of maximum stream function anomalies in the Indian Ocean is located to the north of 60°S (i.e., the latitude of meridional wind anomalies shown in Fig. 7b). While one would not expect a

Fig. 7 Composites of the anomalies of (a) Sea ice extent latitude in degrees, (b) 1000 hPa meridional wind at 60°S (m/s) and (c and d) the 1000 hPa streamfunction anomalies (in $10^6 \text{ m}^2 \text{ s}^{-1}$) for the positive and negative phases of the Southern Annular Mode exceeding one standard deviation. Period 1979–2000, all months of the year used



perfect relationship between wind and ice anomalies, these factors above help explain the asymmetries from the perspective of stationary waves.

The association between the northward (southward) movements of the SIE positioning and the low-level northward (southward) flows of the induced stationary waves can also be seen in other longitudes where significant positive (negative) anomalies of SIE occur. The vertical structure of these stationary waves is barotropic (not shown). The correlation between the meridional wind anomalies and the SIE is $+0.63$ for the positive composite (solid curves) and $+0.58$ for the negative composite (dashed curves).

Figure 8 shows the temporal cross-correlations between the 1000-hPa meridional winds at 60°S at longitude λ_1 and the SIE at longitude λ_2 . These temporal correlations present a new aspect of the associations which fully support the comments above for the association between the meridional wind and the SIE. A consistent positive local correlation is observed, reflecting the contribution of the meridional wind in the north–south migration of SIE at all longitudes as discussed earlier. No doubt the full wind vector, and its implied Ekman drift, result in an ice velocity that advects the ice. In turn, the climatological surface-meridional wind is strongly related to the sea ice as the turning angle of the surface wind on ice motion is relatively

small. The 1000 hPa winds used here are in balance with the geostrophic streamfunction and are very close to the surface winds (the average wintertime MSLP 1000 hPa isobar in the SH lies approximately over 60°S), producing strong correlations. The ocean currents are driven by the surface winds, but on monthly averages there is a large contribution from the stationary waves. In the following sections we discuss the potential role of cyclones and the occurrence of preferential areas for wave amplification, adding to the earlier findings (e.g., Renwick 2002; Kwok and Comiso 2002).

3.3 Cyclone behaviour

In this section we show that one of the physical mechanisms facilitating the climate relations discussed above is given via transient eddy activity, especially meso-cyclones (e.g., polar lows) and synoptic cyclones around Antarctica. Changes in cyclone strength will feedback onto the mean circulation, reinforcing the stationary waves. As noted by Uotila et al. (2009) the resolution of the JRA25 data used in this section is just within the minimum threshold for identifying polar lows, and the automatic tracking scheme is well tuned to capture high frequency variability giving a climate signal that is above noise.

Physical links such as the one hypothesised by high latitude blocking seem to be responsive to key longitudinal variations that can arise from SAM (and ENSO itself), whereas the transient eddies contribute to the maintenance

of the stationary waves that form the blocking. In fact, Yu and Hartmann (1993) found that the shape of the transient eddies changes with the phase of the SAM such that a momentum flux anomaly acts to reinforce the jet vacillations, while Magnusdottir et al. (2004) explored the impacts of changes in SST and SIE on the NAM. The SD/DP fields discussed in this section presents a spatially inhomogeneous response when compared to the mean field (e.g., MSLP), helping to understand the integrated role that the transient eddies within the synoptic systems play in the climate maintenance, advancing further from the recent results of Stammerjohn et al. (2008) and Yuan and Li (2008).

It is important that we cover this gap because cyclone behaviour and their intrinsic momentum and heat fluxes play a fundamental role in displacing large amounts of sea ice either directly via wind stress or indirectly via changes in the air-sea heat fluxes and in the oceanic circulation. This effect has been shown to play a fundamental role in the strong SIE decline observed in the NH where the sea ice is thinner (Rothrock et al. 1999; Stroeve et al. 2005, 2007; Serreze et al. 2003, 2007; IPCC 2007; Simmonds et al. 2008; Simmonds and Keay 2009). Based on the results discussed in Figs. 3 and 4 we concentrate on the relationships during the SH summer period when both SAM and SIE have positive trends. We note, however, that all the relationships discussed between SIE and SAM/ENSO until now have been considered involving all months of the year, as the overall pattern is not season dependent. The only region in terms of SIE that shows a somewhat marked seasonal contrast in the SAM/ENSO response is the eastern Weddell Sea. This is discussed separately in Sect. 3.4.

As discussed in Sect. 2 we use two pertinent cyclone statistics indicators, viz., the SD as representative of the total cyclone amount per given area and the DP as a representation of cyclone intensity. These variables characterise the role that individual synoptic systems play in climate. Figure 9 shows the DJF (a) SD and (b) DP anomalies associated with the top five minus the bottom five AAOI events during the period 1979–2008. The results are masked over the continents in order to retain only the mid and high latitude signal of relevance for sea ice displacement. As noted by Pezza et al. (2008) standard significance tests tend to be very patchy for this type of analysis because of the high variability associated with cyclones, even when the response is robust and spatially organised. The coloured values above a magnitude of unity are of meteorological significance, being of the same order of magnitude as the standard deviation at mid-latitudes. They show the areas where the eddy characteristics differ significantly with the phase of the AAOI.

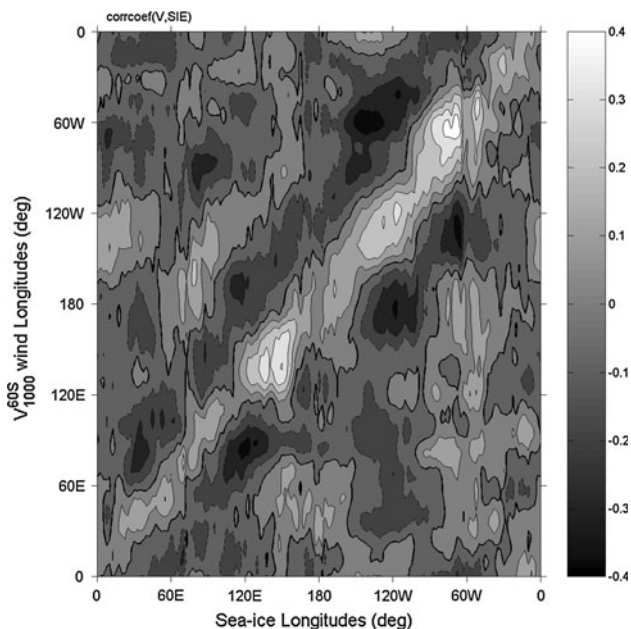


Fig. 8 Cross-correlations between the Sea Ice Edge anomalies and the 1000 hPa meridional winds (m s^{-1}) at 60°S as a function of longitude. Period 1979–2000, all months of the year used

The primary cause for the maximum band in both SD and DP around Antarctica in Fig. 9 is the displacement of the circumpolar trough that shifts to the south when the SAM is positive. This effect, in principle, responds to the general circulation of the atmosphere and should be somehow independent of the sea ice. However, in the real world this pattern interacts with the sea ice present in the region, and both the trough and the sea ice respond to each other's presence in a non-linear way. The overall structure of the band of maximum cyclone activity is similar in terms of SD and DP, but regional differences arise

depending on the geography of the Antarctic continent. For instance, in the Weddell Sea both areas of maximum SD and DP coincide, indicating that more cyclones occur in the area during the positive phase of the SAM, and also that those cyclones are on average deeper than normal. On the Amundsen Sea, however, although there are more cyclones when the SAM is positive they are not more intense than average. This could be a result of those cyclones being relatively short lived, migrating to the Bellingshausen Sea and intensifying over there. Indirectly this can also be a reflection that there is less sea ice available in the area to reinforce the cyclogenesis.

From Fig. 9a we observe a very clear and well organised pattern with positive SD anomalies around Antarctica and negative anomalies over mid-latitudes in a pattern that resembles the MSLP signature associated with the SAM. It is also evident that the SD pattern is not as annular as the EOF structure earlier discussed in Fig. 1a. The spatial asymmetries in Fig. 9 are of direct importance for the variability earlier discussed in the sea ice latitudes. The DP field (Fig. 9b) shows that most of the areas subject to higher cyclone frequency are also host to stronger cyclones when the SAM is positive. This produces reinforcement back on the mean structure, meaning that more and stronger cyclones will strengthen the anomalous atmospheric conditions that will project more strongly onto the positive SAM. As discussed earlier, DP is a very informative cyclone statistic which is not influenced by large scale changes in background pressure. Hence the greater depths found around the Subantarctic do not come about as a simple response to the lower mean pressure during positive SAM events.

Another aspect to consider is that the sea ice response to the SAM can also be partially understood via the SST and surface air anomalies induced by the SAM. In fact, the signatures in sea ice, SST and surface air temperatures are very similar (Karpechko et al. 2009). Changes in the air or ocean temperature may also be linked to changes in cyclone properties. In addition to the dynamic effects of cyclone activity (ice drift) there will also be thermodynamic effects such as changes in heat advection (both in the atmosphere and near-surface ocean) as well as air-sea fluxes. Another issue that is not covered in our analyses is the long term sea ice response to the SAM, via enhanced eddy activity in the ocean (Screen et al. 2009).

The high cyclogenesis around Antarctica can also be due to convergence associated with katabatic winds near the coast (Carrasco et al. 2003). Those strong winds tend to converge over areas with strong SST gradient between the free ocean and the ice covered ocean, with dramatic changes in albedo and heat fluxes (Simmonds et al. 2003; Carrasco et al. 2003). We argue that the mesoscale processes such as the katabatic winds tend to be more effective

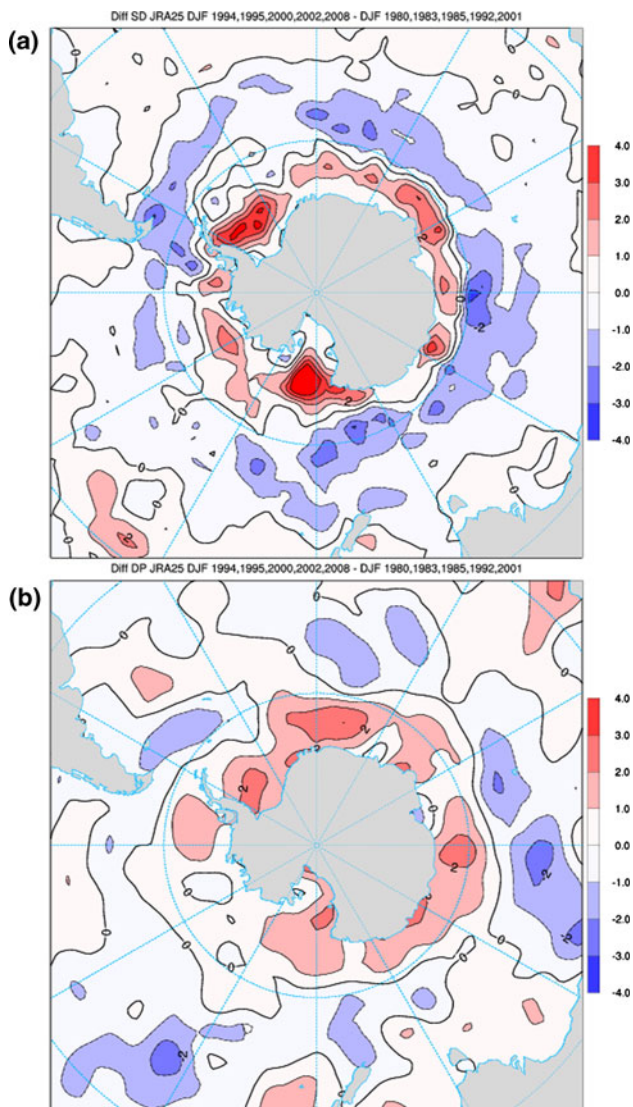


Fig. 9 a Cyclone density (SD) and b depth (DP) associated with the top five minus the bottom 5 years of the Antarctic Oscillation Index during December–January–February. Top 5 years: 1994, 1995, 2000, 2002, **2008**, and bottom 5 years: **1980**, **1983**, 1985, 1992, 2001. JRA25 dataset is used for period 1979–2008, and ‘year’ refers to the year when the season finishes. SD is given in 10^3 (deg.lat)², and DP is given in hPa. Coincident years with SIE extremes are indicated in bold. See text for more details

in reducing the central pressure of each cyclone forming in the region when the large scale (SAM) is favourable (i.e., more robust circumpolar troughs when the SAM is positive). From a larger perspective the katabatic winds tend to respond to the proximity and intensity of the circumpolar trough via enhanced subsidence over the plateau and enhanced ascending motion off the coast (Parish and Bromwich 2007). We argue that Fig. 9 offers a good example of this increased relationship during the positive polarity of the SAM as reflected by the increased offshore cyclogenesis.

Figure 10 shows the (a) SD and (b) DP anomalies associated with the top five minus the bottom five SIE years. Although there were a few cases in which an anomalous year for the SAM composite was also identified

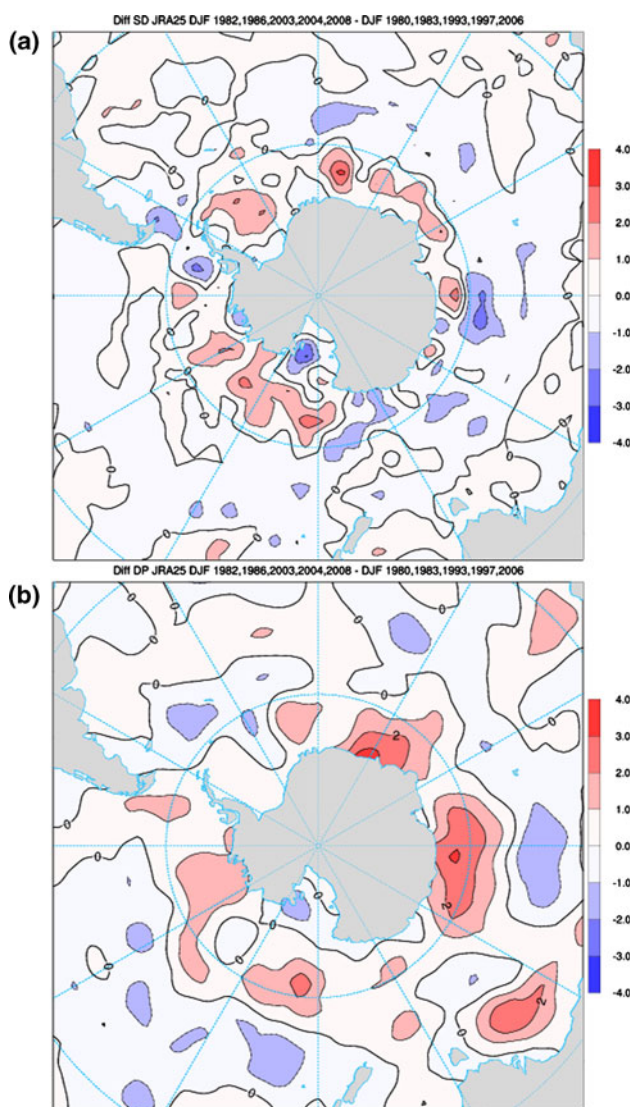


Fig. 10 As in Fig. 9, but for Sea Ice Extent years. Top 5 years: 1982, 1986, 2003, 2004, **2008**, and bottom 5 years: **1980**, **1983**, 1993, 1997, 2006. Coincident years with SAM extremes are indicated in bold

as an anomalous SIE year, the samples are reasonably independent (see figure caption for details). It is interesting that, notwithstanding this relative independence, the cyclone behaviour for SIE and SAM composites bear some similarity in the broadest sense, particularly over high latitudes. The mid-latitude signal is very pronounced for the SAM but weak for the SIE, particularly with the SD field.

There is an interesting aspect to the response above. Simmonds and Wu (1993) showed via model simulations that a greater SIE will decrease the number of cyclones around Antarctica. Although their analysis was performed for winter, Raphael (2003) found a similar result for summer. Figure 10 suggests the opposite, i.e., more and deeper subantarctic cyclones when there is more sea ice. This apparent paradox is resolved when one realises that those model studies just considered the effects of SIE changes on the atmosphere without including feedbacks. Physically, stronger cyclones will push more sea ice out of the formation region much more effectively, and hence push the edge equatorward. As the Antarctic region is cold enough to produce substantial re-freezing and more ice generation further south, the overall effect of stronger cyclones is to increase the SIE, differently to the NH where more intense cyclones during the summer can lead to a rapid break up and reduction of SIE (Simmonds et al. 2008; Simmonds and Keay 2009).

We note that the longitudes of maximum correlation discussed in Fig. 6 are also areas of intense cyclone anomalies, and this is also observed in the ENSO response (not shown). The ENSO signature associated with the cyclone anomalies resembles the anomalies associated during the extremes in the SAM, being somewhat less zonally symmetric (see, e.g., Pezza et al. 2008). As discussed earlier this similarity in the ENSO/SAM response is not surprising when one considers the possibility of preferential areas for stationary wave amplification around the Antarctic continent. This fact is reflected by the apparent mirroring relationship in Fig. 6. As noted previously, regardless of these similarities in their final responses ENSO and SAM may arise from completely different types of forcing. The apparent synergy in the ENSO/SAM response is discussed in more detail in the next section, when additional considerations are made based on the exceptional sea ice and SAM conditions recorded during the SH summer of 2008.

3.4 Summer 2008 in climate context

Our analyses agree with Sen Gupta and England (2006) who showed that the sea ice response to SAM would be negative in the regions where the sea ice edge is aligned north-eastward, as anomalous eastward advection in this

case would lead to ice field contraction. While explaining negative sea ice response to the SAM one also needs to consider the possibility of ice melting due to anomalous advection of warm air. The highest on record summer of 2007/2008 with respect to the SAM and SIE (Fogt et al. 2008) offers the opportunity to gain further insight on the physical relationships between these parameters, and is worth putting in climate context. This year presented the highest AAOI ever recorded for the season (about +1.5) by a far margin, corresponding to about two standard deviations above the average (compare with the one standard deviation lines shown in Fig. 3). An alternative AAOI definition based on surface station data (Marshall 2003) captures the summer 2008 as second highest on record presumably because of the relatively poor coverage of stations in relation to the spatial distribution of the largest anomalies observed during that year (not shown).

Figure 11 shows the spatial distribution of (a) SIE and (b) sea ice concentration anomalies during December 2007. Although most of the areas around Antarctica presented larger SIE than average the pattern is not uniform, i.e., large sectorial variations are seen in both extent and concentration. The nature of the spatial variations in the anomalous fields observed in December 2007 strongly resembles the correlations between the latitudes of SIE and SAM depicted in Fig. 6, with negative SIE and negative concentration anomalies occurring over the Bellingshausen Sea, and positive anomalies occurring over the eastern Ross Sea, the Southern Ocean sector to the south of Australia and the eastern Indian Ocean. Those key areas are indicated by black arrows in Fig. 11, whose direction indicates the direction of the anomalous SIE movement (annually taken) when the SAM is positive.

The Weddell Sea also presented strong anomalies, and SIE in this sector is positively correlated with SAM only during the summer (Fig. 7 of Lefebvre et al. 2004). This is why the annual association with SAM for the Weddell is small in our Fig. 6. We note that the Weddell sector also tends to hold more sea ice during La Niña years in the summer season only, with an opposite effect observed throughout the rest of the year (Fig. 7 of Kwok and Comiso 2002). This is also seen in Fig. 6, where a small area within the Weddell Sea is positively correlated with temperatures over the Niño 3.4 on an annual basis. As December 2007 presented a moderate (non-canonical) La Niña it is likely that ENSO and SAM acted in concert to increase the SIE in the Weddell sector as well, while we note that this particular response in the Weddell is only observed over the summer months.

From the discussions above it is apparent that a combination of La Niña and positive SAM or El Niño and negative SAM will generally tend to reinforce the same large scale pattern of sea ice anomalies irrespective of the

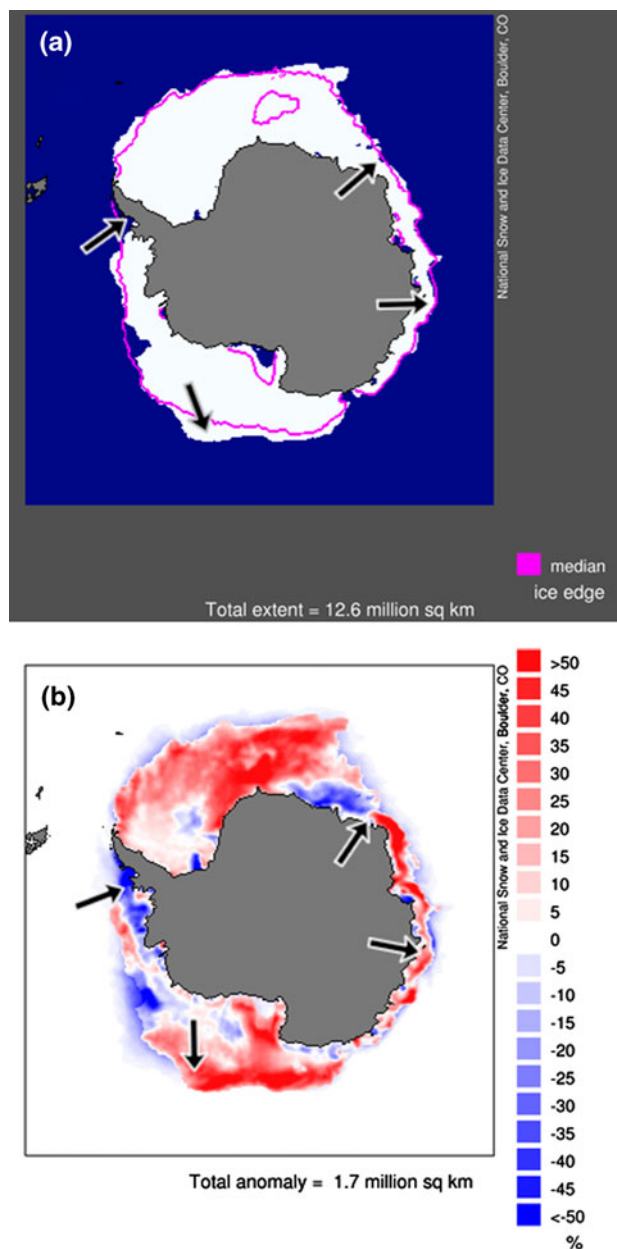


Fig. 11 a Sea ice extent and b sea ice concentration anomalies for December 2007. The arrows indicate the direction of the anomalies given by the correlation shown in Fig. 6 for the positive SAM polarity. Concentration units in anomalous percentage. See text for further details

season, in agreement with Liu et al. (2004) and Wheeler (2008). We also note that Stammerjohn et al. (2008) found that the SAM and ENSO influences on western Antarctic Peninsula were out of phase in the 1980s and in phase in the 1990s, therefore non-linearity and other influences can be part of the associations here discussed. As discussed earlier, one of the aspects adding to the complexity in the system is that the trends in SAM cannot fully explain the trends in SIE for the extent of the current dataset. The

greatest responses seem to occur when the combined influences of SAM and ENSO coincide and reinforce the same wave pattern, as the Pacific South American pattern would indicate. The SIE anomalies during the record breaking summer of 2008 seem to have reflected well these general climate associations.

It is of interest to compare the patterns discussed above with the long term spatial distribution of sea ice concentration trends during the month of January, as this is the month when the SAM has its greatest positive trend. From Fig. 12 we can see that the long term trend in ice concentration resembles the pattern observed during December 2007, with negative trends in the Bellingshausen Sea and positive trends over the areas where there is positive correlation between SIE and SAM. The areas of maximum correlation are given by the direction of the arrows as in Fig. 11. These trends reinforce the idea that the overall positive increase in the sea ice during the southern summer has been consistent with the changes observed in the SAM during the same period. However, this view is not intended to be quantitative, as the natural climate variability within the period of analysis is greater than the signal from the trends. In other words, the reliable period of SAM and SIE data available is still too short to allow us to give an estimate of how much of the changes in sea ice can be directly attributed to the SAM.

Figure 13 shows the SD (a) and DP (b) anomalies observed during the summer 2008. From Fig. 13a a clear

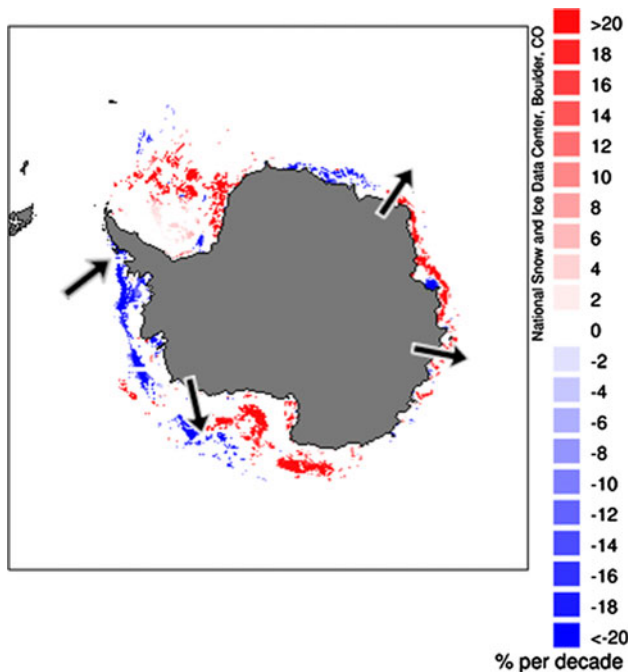


Fig. 12 Long term trend in sea ice concentration anomalies (% per decade) for January, with the *arrows* similar to Fig. 11. Period 1979–2008 used

pattern with positive anomalies around Antarctica and negative anomalies over mid-latitudes is seen. This pattern resembles the positive SAM signature shown in Fig. 9. The DP behaviour (b) also shows positive anomalies over most of high latitudes with some elements resembling the positive SAM and SIE discussed earlier (Figs. 9b and 10b) but also suggesting a higher degree of spatial variability. A comparison between Figs. 13 and 11 reveals that the most intense cyclone SD anomalous areas occurred adjacent to the areas where the ice anomalies were maximised. As demonstrated for the NH (Simmonds et al. 2008; Simmonds and Keay 2009), this points to the importance of the transient eddy activity in influencing the ice displacement, where the large scale pattern seems to be fundamentally

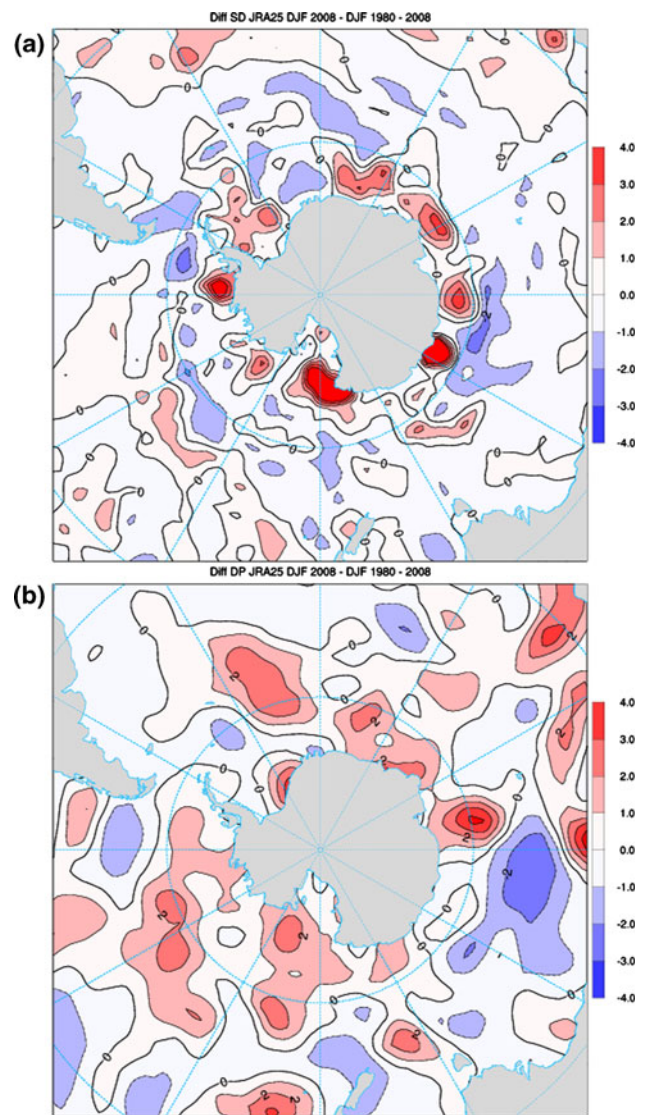


Fig. 13 a Cyclone density (SD) and b depth (DP) anomalies for December–January–February 2008. JRA25 dataset, period 1979–2008 as climatology reference is used. SD is given in 10^3 (deg.lat)², and DP is given in hPa

driven by the SAM. Future analyses with many more years of data would be able to greatly tighten these associations.

4 Concluding remarks

In this paper we have addressed the association between the SAM and the hemispheric climate variability through impacts on the sea ice via stationary waves and cyclone anomalies. The southern sea ice has shown modest increases and established new record ice coverage in the summer of 2008 by a wide margin, raising questions on how this peculiar behaviour would fit with the sharp decline observed in the NH as the effects of global warming become more evident.

We show that the SAM and the SIE are significantly correlated over several regions annually, the most important being the Bellingshausen/west Weddell Seas, the Atlantic/Indian sector, the Southern Ocean to the southwest of Australia and the South Pacific to the east of the Ross Sea. The correlations are positive for all areas with exception of the Bellingshausen/west Weddell, meaning that when all effects are taken into consideration an overall ice increase is associated with the SAM's positive polarity. When ENSO effects are taken into account a mirroring relationship to that observed between SAM and sea ice is observed over most longitudes. This implies that ENSO and SAM would act in synergy at least as far as the synoptic effects are concerned, but we also note that the original forcings for SAM and ENSO are quite different. La Niña years with positive SAM would present the most favourable conditions for overall ice growth (except to the west of the Antarctic Peninsula where the opposite is seen). However, as noted by Khokhlov et al. (2006) and Stammerjohn et al. (2008) the role of non-linearity is also important in that the combined impacts of SAM and ENSO may change on a multi-decadal time scale.

We formed a hypothesis involving meridional advection via stationary Rossby waves. These waves tend to resonate with greater amplitude over preferential longitudes around Antarctica when and where more intense polar cyclones are observed, suggesting a synergy between stationary wave processes and transient eddies. Our cyclone behaviour analysis suggests that the interaction between transient eddies and stationary waves is of marked importance, acting to reinforce the atmospheric anomalies observed during the anomalous phases of the SAM. We speculate that parts of this response may reflect fundamental high-latitude modes where most of the energy gets dispersed, responding to the shape of the Antarctic continent and to the spatial distribution of ocean currents and heat fluxes.

In terms of trends, the combination of record sea ice, record SAM and La Niña in the southern summer of 2008

mimicked well the climate relationships discussed above, stressing the importance of SAM and ENSO acting together in synergy (L'Heureux and Thompson 2006). As discussed above, this is not to imply that SAM and ENSO originate from the same process (as indeed they don't), but it fits well with the idea of "synchronous variability" (Hall and Visbeck 2002) in that there is a large response when both influences act in concert. We also note that within the period of reliable data in the SH the magnitude of the natural variability is greater than the magnitude of the trends. A longer period of analysis would be required in order to unequivocally determine the individual amounts of contribution from SAM or ENSO on the sea ice trends.

An eventual reversal in the currently positive SH sea ice trends has been predicted by most of the IPCC A4 climate models, which show significant losses (ranging from 10 to 50%) towards the end of the twenty-first century in both summer and winter (Sen Gupta et al. 2009). A reduction in SIE can be understood as associated with global warming even if the variability in the SAM and ENSO remains unchanged. A key player in this chain of events is the potent effect that strong cyclones have of breaking down the ice, as has been demonstrated for the NH (Simmonds et al. 2008; Simmonds and Keay 2009). Although in the SH the polar latitudes are still cold enough to allow for a rapid re-freeze and further ice generation, our cyclone analysis clearly shows that the areas of stronger polar cyclones are also areas of maximised sea ice displacement.

Acknowledgments The authors would like to acknowledge the Australian Research Council and the Antarctic Science Advisory Committee for funding parts of this work. We thank Drs. Matthew Wheeler, James Screen and Petteri Uotila for invaluable comments on an early version of this manuscript. We also thank the National Snow and Ice Data Center (NSIDC) and Dr. Phil Reid for making their data and analyses publicly available. Comments by two anonymous reviewers contributed to further improve this text.

References

- Baines PG, Fraedrich K (1989) Topographic effects on the mean tropospheric flow patterns around Antarctica. *J Atmospheric Sci* 46:3401–3415
- Cai W, Shi G, Cowan T, Bi D, Ribbe J (2005) The response of the Southern Annular Mode, the East Australian Current, and the Southern mid-latitude ocean circulation to global warming. *Geophys Res Lett* 32. doi:10.1029/2005GL024701
- Carrasco JF, Bromwich DH, Monaghan AJ (2003) Distribution and characteristics of mesoscale cyclones in the Antarctic: Ross Sea eastward to the Weddell Sea. *Mon Wea Rev* 131:289–301
- Cohen J, Barlow M (2005) The NAO, the AO, and global warming: how closely related? *J Clim* 18:4498–4513
- Comiso JC, Nishio F (2008) Trends in the sea ice cover using enhanced and compatible AMSR-E, SSM/I, and SMMR data. *J Geophys Res* 113, C02S07. doi:10.1029/2007C004257
- Fogt RL, Bromwich DH (2006) Decadal variability of the ENSO teleconnection to the high latitude South Pacific governed by coupling with the Southern Annular Mode. *J Clim* 19:979–997

- Fogt RL, Bromwich DH, Hines KM (2008) Recent SAM and ENSO teleconnections for Antarctica. *US CLIVAR Var* 6(1):4–6
- Fogt RL, Perlwitz J, Monaghan A, Bromwich DH, Jones J, Marshall GJ (2009) Historical SAM Variability. Part II: 20th century variability and trends from reconstructions, observations, and the IPCC AR4 models. *J Clim* 22:5346–5365
- Fyfe JC, Boer GJ, Flato GM (1999) The Arctic and Antarctic Oscillations and their projected changes under global warming. *Geophys Res Lett* 26:1601–1604
- Gloersen P, Campbell W, Cavalieri D, Comiso JC, Parkinson CL, Zwally J (1992) Arctic and Antarctic sea ice, 1978–1987: satellite passive-microwave observations and analysis. National Aeronautics and Space Administration (NASA), 511. Special Publication, Washington, DC, pp 1–290
- Godfred-Spenning CR, Simmonds I (1996) An analysis of Antarctic sea ice and extratropical cyclone associations. *Int J Climatol* 16:1315–1332
- Gong DY, Wang SW (1999) Definition of Antarctic Oscillation index. *Geophys Res Lett* 26:459–462
- Hall A, Visbeck M (2002) Synchronous variability in the Southern Hemisphere atmosphere, Sea ice, and Ocean resulting from the Annular Mode. *J Clim* 15:3043–3057
- Hendon HH, Thompson DWJ, Wheeler MC (2007) Australian Rainfall and Surface Temperature Variations Associated with the Southern Annular Mode. *J Clim* 20:2452–2467
- Herweijer C, Seager R (2008) The global footprint of persistent extratropical drought in the instrumental era. *Int J Climatol* 28:1761–1774. doi:10.1002/joc.1590
- Holland MM, Raphael MN (2006) Twentieth century simulation of the Southern Hemisphere climate in coupled models. Part II: Sea ice conditions and variability. *Clim Dyn* 26:229–245. doi:10.1007/s00382-005-0087-3
- Hurrell JW (1995) Decadal trends in the North Atlantic Oscillation region temperatures and precipitation. *Science* 269:676–679
- IPCC (2007) Climate change 2007: the physical science basis. Contribution of working group I to the fourth assessment report of the intergovernmental panel on climate change. In: Solomon S, Qin D, Manning M, Chen Z, Marquis M, Averyt KB, Tignor M, Miller HL (eds). Cambridge University Press, Cambridge
- Jones DA, Simmonds I (1993) A climatology of Southern Hemisphere extratropical cyclones. *Clim Dyn* 9:131–145
- Kanamitsu M, Ebisuzaki W, Woollen J, Yang SK, Hnilo JJ, Fiorino M, Potter GL (2002) NCEP-DOE AMIP-II reanalysis (R-2). *Bull Am Meteorol Soc* 83:1631–1643
- Karpechko A, Gillett NP, Marshall GJ, Screen JA (2009) Climate impacts of the Southern Annular Mode simulated by the CMIP3 models. *J Clim* 22:3751–3768
- Khokhlov VN, Glushkov AV, Loboda NS (2006) On the nonlinear interaction between global teleconnection patterns. *Q J R Meteorol Soc* 132:447–465
- Kidston J, Renwick JA, McGregor J (2009) Hemispheric-scale seasonality of the Southern Annular Mode and impacts on the climate of New Zealand. *J Clim* 22:4759–4770
- Krüger K, Naujokat B, Labitzke K (2005) The unusual midwinter warming in the Southern Hemisphere Stratosphere 2002: a comparison to Northern Hemisphere Phenomena. *J Atmos Sci* 62:603–613
- Kwok R, Comiso JC (2002) Southern Ocean climate and sea ice anomalies associated with the Southern Oscillation. *J Clim* 15:487–501
- L'Heureux ML, Thompson DWJ (2006) Observed relationships between the El Niño–Southern Oscillation and the extratropical zonal-mean circulation. *J Clim* 19:276–287
- Lau KM, Sheu PJ, Kang IS (1994) Multiscale low-frequency circulation modes in the global atmosphere. *J Atmos Sci* 51:1169–1193
- Lefebvre W, Goosse H, Timmermann R, Fichefet T (2004) Influence of the Southern Annular Mode on the sea ice–ocean system. *J Geophys Res* 109. doi:10.1029/2004JC002403
- Lim E-P, Simmonds I (2007) Southern Hemisphere winter extratropical cyclone characteristics and vertical organization observed with the ERA-40 data in 1979–2001. *J Clim* 20:2675–2690
- Liu J, Curry JA, Martinson DG (2004) Interpretation of recent Antarctic sea ice variability. *Geophys Res Lett* 31:L02205. doi:10.1029/2003GL018732
- Lovenduski NS, Gruber N (2005) Impact of the Southern Annular Mode on Southern Ocean circulation and biology. *Geophys Res Lett* 32. doi:10.1029/2005GL022727
- Magnusdottir G, Deser C, Saravanan R (2004) The effects of North Atlantic SST and sea ice anomalies on the winter circulation in CCM3. Part I: Main features and storm track characteristics of the response. *J Clim* 17:857–876
- Marshall GJ (2003) Trends in the Southern Annular Mode from observations and reanalyses. *J Clim* 16:4134–4143
- Mbatha N, Sivakumar V, Malinga SB, Bencherif H, Pillay SR (2010) Study on the impact of sudden stratosphere warming in the upper mesosphere–lower thermosphere regions using satellite and HF radar measurements. *Atmos Chem Phys* 10:3397–3404
- Meneghini B, Simmonds I, Smith IN (2007) Association between Australian rainfall and the Southern Annular Mode. *Int J Climatol* 27:109–121. doi:10.1002/joc.1370
- Murray RJ, Simmonds I (1991) A numerical scheme for tracking cyclone centres from digital data. Part I: development and operation of the scheme. *Aust Meteorol Mag* 39:155–166
- Onogi K, Tsutsui J, Koide H, Sakamoto M, Kobayashi S, Hatsushika H, Matsumoto T, Yamazaki N, Kamahori H, Takahashi K, Kadokura S, Wada K, Kato K, Oyama R, Ose T, Mannoji N, Taira R (2007) The JRA-25 reanalysis. *J Meteor Soc Jpn* 85:369–432
- Parish TR, Bromwich DH (2007) Reexamination of the near-surface airflow over the Antarctic continent and implications on atmospheric circulations at high latitudes. *Mon Wea Rev* 135:1961–1973
- Parkinson CL (2004) Southern Ocean sea ice and its wider linkages: insights revealed from models and observations. *Antarct Sci* 16:387–400
- Pezza AB, Durrant TH, Simmonds I, Smith I (2008) Southern Hemisphere synoptic behaviour in extreme phases of SAM, ENSO, sea ice extent and southern Australia rainfall. *J Clim* 21:5566–5584
- Raphael MN (2003) Impact of observed sea-ice concentration on the Southern Hemisphere extratropical atmospheric circulation in summer. *J Geophys Res* 108. doi:10.1029/2002JD003308
- Rashid HA, Simmonds I (2004) Eddy-zonal flow interactions associated with the Southern Hemisphere annular mode: results from NCEP-DOE reanalysis and a quasi-linear model. *J Atmospheric Sci* 61:873–888
- Renwick JA (1998) ENSO-related variability in the frequency of South Pacific blocking. *Mon Weather Rev* 126:3117–3123
- Renwick JA (2002) Southern Hemisphere circulation and relations with sea ice and sea surface temperature. *J Clim* 15:3058–3068
- Renwick JA (2004) Trends in the Southern Hemisphere polar vortex in NCEP and ECMWF reanalyses. *Geophys Res Lett* 31, L07209. doi:10.1029/2003GL019302
- Roscoe HK, Haigh JD (2007) Influences of ozone depletion, the solar cycle and the QBO on the Southern Annular Mode. *Quart J R Met Soc* 133:1855–1864
- Rothrock DA, Yu Y, Maykut GA (1999) Thinning of the Arctic sea-ice cover. *Geophys Res Lett* 26:3469–3472
- Screen JA, Gillett NP, Stevens DP, Marshall GJ, Roscoe HK (2009) The role of eddies in the Southern Ocean temperature response to the Southern Annular Mode. *J Clim* 22:806–818

- Sen Gupta A, England MH (2006) Coupled ocean-atmosphere-ice response to variations in the Southern Annular Mode. *J Clim* 19:4457–4486
- Sen Gupta A, Santoso A, Taschetto AS, Ummerhofer CC, Trevena J, England MH (2009) Projected changes to the Southern Hemisphere ocean and sea-ice in the IPCC AR4 climate models. *J Clim* 22:3047–3078
- Serreze M, Maslanik JA, Sacmbos TA et al. (2003) A record minimum Arctic sea ice extent and area in 2002. *Geophys Res Lett* 30. doi:10.1029/2002GL016406
- Serreze MC, Holland MM, Stroeve J (2007) Perspectives on the Arctic's shrinking sea ice cover. *Science* 315:1533–1536
- Shindell DT, Schmidt GA (2004) Southern Hemisphere climate response to ozone changes and greenhouse gas increases. *Geophys Res Lett* 31. doi:10.1029/2004GL020724
- Simmonds I (2003a) Regional and large-scale influences on Antarctic Peninsula Climate. *AGU Antarct Res Ser* 79:31–42
- Simmonds I (2003b) Modes of atmospheric variability over the Southern Ocean. *J Geophys Res* 108:8078. doi:10.1029/2000JC000542
- Simmonds I, Budd WF (1991) Sensitivity of the Southern Hemisphere Circulation to leads in the Antarctic Pack Ice. *Q J R Meteorol Soc* 117:1003–1024
- Simmonds I, Hope P (1997) Persistence characteristics of Australian rainfall anomalies. *Int J Climatol* 17:597–613
- Simmonds I, Jacka TH (1995) Relationships between the interannual variability of Antarctic sea ice and the Southern Oscillation. *J Clim* 8:637–646
- Simmonds I, Keay K (2000) Variability of Southern Hemisphere extratropical cyclone behaviour, 1958–1997. *J Clim* 13:550–561
- Simmonds I, Keay K (2009) Extraordinary September arctic sea ice reductions and their relationships with storm behaviour over 1979–2008. *Geophys Res Lett* 39:L19715. doi:10.1029/2009GL039810
- Simmonds I, Wu X (1993) Cyclone behaviour response to changes in winter Southern Hemisphere sea-ice concentration. *Q J R Meteorol Soc* 119:1121–1148
- Simmonds I, Keay K, Lim E-P (2003) Synoptic activity in the seas around Antarctica. *Mon Weather Rev* 131:272–288
- Simmonds I, Rafter A, Cowan T, Watkins A, Keay K (2005) Large scale vertical momentum, kinetic energy and moisture fluxes in the Antarctic sea-ice region. *Boundary Layer Meteorol* 117:149–177
- Simmonds I, Burke C, Keay K (2008) Arctic climate change as manifest in cyclone behaviour. *J Clim* 21:5777–5796. doi:10.1175/2008JCLI2366.1
- Stammerjohn SE, Martinson DG, Smith RC, Yuan X, Rind D (2008) Trends in Antarctic annual sea ice retreat and advance and their relation to El Niño–Southern Oscillation and Southern Annular Mode variability. *J Geophys Res* 113, C03S90, 20 pp. doi:10.1029/2007JC004269
- Stroeve JC, Serreze MC, Fetterer F et al (2005) Tracking the Arctic's shrinking ice cover: another extreme September minimum in 2004. *Geophys Res Lett* 32:L04501. doi:10.1029/2004GL02810
- Stroeve J, Holland MM, Meier W, Scambos T, Serreze M (2007) Arctic ice decline: faster than forecast. *Geophys Res Lett* 34. doi:10.1029/2007GL029703
- Thompson DW, Solomon S (2002) Interpretation of recent Southern Hemisphere climate change. *Science* 296:895–899
- Thompson DW, Wallace JM (2000) Annular modes in the extratropical circulation. Part I: month-to-month variability. *J Clim* 13:1000–1016
- Thompson DWJ, Wallace JM, Hegerl GC (2000) Annular modes in the extratropical circulation. Part II: trends. *J Clim* 13:1018–1036
- Turner J (2004) The El Niño–Southern Oscillation and Antarctica. *Int J Climatol* 24:1–31
- Turner J, Overland JE, Walsh JE (2007) An Arctic and Antarctic perspective on recent climate change. *Int J Clim* 27, 277–293. doi:10.1002/joc.1406
- Uotila J (2001) Observed and modeled sea-ice drift response to wind forcing in the northern Baltic Sea. *Tellus* 53A:112–128
- Uotila J, Vihma T, Launiainen J (2000) Response of the Weddell Sea pack ice to wind forcing. *J Geophys Res* 105:1135–1151
- Uotila P, Pezza AB, Cassano JJ, Keay K, Lynch AH (2009) A comparison of low pressure system statistics derived from a high-resolution NWP output and three reanalysis products over the Southern Ocean. *J Geophys Res* 114:1–19, Art No. D17105. doi:10.1029/2008JD011583
- Uppala SM, Kållberg PW, Simmons AJ, Andrae U, Da Costa Bechtold V, Fiorino M, Gibson JK, Haseler J, Hernandez A, Kelly GA, Li X, Onogi K, Saarinen S, Sokka N, Allan RP, Andersson E, Arpe K, Balmaseda MA, Beljaars ACM, Van De Berg L, Bidlot J, Bormann N, Caires S, Chevallier F, Dethof A, Dragosavac M, Fisher M, Fuentes M, Hagemann S, Hólm E, Hoskins BJ, Isaksen I, Janssen PAEM, Jenne R, McNally AP, Mahfouf J-F, Morcrette J-J, Rayner NA, Saunders RW, Simon P, Sterl A, Trenberth KE, Untch A, Vasiljevic D, Viterbo P, Woollen J (2005) The ERA-40 Reanalysis. *Q J R Meteorol Soc* 131:2961–3012
- Wang J, Zhang J, Watanabe E, Ikeda M, Mizobata K, Walsh JE, Bai X, Wu B (2009) Is the Dipole anomaly a major driver to record lows in Arctic summer sea ice extent? *Geophys Res Lett* 36, L05706. doi:10.1029/2008GL036706
- Watkins AB, Simmonds I (2000) Current trends in Antarctic sea ice: the 1990s impact on a short climatology. *J Clim* 13:4441–4451
- Wheeler MC (2008) Seasonal climate summary Southern Hemisphere summer 2007–08: Mature La Niña, an active MJO, strongly positive SAM, and highly anomalous sea ice. *Aust Meteor Mag* 57:379–393
- Yu J-Y, Hartmann DL (1993) Zonal flow vacillation and eddy forcing in a simple GCM of the atmosphere. *J Atmospheric Sci* 50:3244–3259
- Yuan X, Li C (2008) Climate modes in southern high latitudes and their impacts on Antarctic sea ice. *J Geophys Res* 113, C06S91, 13 pp. doi:10.1029/2006JC004067
- Yuan XJ, Martinson DG (2000) Antarctic sea ice extent variability and its global connectivity. *J Clim* 13:1697–1717
- Zwally HJ, Comiso JC, Parkinson CL, Cavalieri DJ, Gloersen P (2002) Variability of Antarctic sea ice 1979–1998. *J Geophys Res* 107:3041. doi:10.1029/2000JC000733